NASA CONTRACTOR
REPORT

NASA CR-987

NASA CR-987

STUDY OF DENSITY
CALIBRATION IN SPACE

by P. Fowler and F. J. Brock

Prepared by
NATIONAL RESEARCH CORPORATION
Cambridge, Mass.
for Goddard Space Flight Center

NATIONAL AERONAUTICS AND SPACE ADMINISTRATION • WASHINGTON, D. C. • DECEMBER 1967

STUDY OF DENSITY CALIBRATION IN SPACE

By P. Fowler and F. J. Brock

FOREWORD

This Final Report covers the work performed under contract NAS5-3959 from 29 June, 1966 to 16 January, 1967.

The contract with National Research Corporation, Cambridge, Massachusetts was initiated by National Aeronautics and Space Administration, Goddard Space Flight Center for the "Study of Density Calibration in Space". Mr. George P. Newton (Code 651) of the Goddard Space Flight Center, Greenbelt, Maryland was technical monitor.

The research covered in this report was carried out by Peter Fowler (Principal Investigator) and Frank J. Brock.

TABLE OF CONTENTS

PAGE

LIST OF FIGURES

LIST OF TABLES

STUDY OF DENSITY CALIBRATION IN SPACE

By P. Fowler and F. J. Brock
National Research Corporation

1. SUMMARY

Methods of calibrating ion gauges and mass spectrometers were studied, under NASA Contract NAS5-3959, to determine a method which would be applicable to in-flight calibration of detectors installed on space craft. The method developed in the first phase of the program, consists of diffusing a known hydrogen flux through the wall of a small diffuser tube into the detector enclosure which produces a pressure increment equal to the ratio of hydrogen flux to exhaust conductance, by raising the temperature of the tube with an internal heater which dissipates a prescribed power for a prescribed time interval. In the first phase of the work, three successive generations of prototype in-flight calibrators were designed and constructed and the performance of the Mark I and Mark II were experimentally evaluated. The performance of Mark III has been evaluated in the second phase of the program.

The results indicate that the diffuser generates a hydrogen flux which is linear over a dynamic range of 3×10^5, that calibration pulse heights are repeatable within $\pm 2.0\%$ and that pulse height variation can be maintained less than 1.0% for 30 seconds. The data indicate that the pressure decay rate, associated with the diffuser, following a calibration pulse is such that after 15 minutes the pressure is no more than several percent of the external pressure if the calibration pulse is no more than an order of magnitude above the external pressure, except for pressures less than 10^{-9} Torr, which require a longer recovery time. Recommendations are made for shortening the low pressure recovery time.

2. INTRODUCTION

During the first phase of this program a method was developed which is applicable to the calibration of ion gauges and mass

spectrometers during space flight. The method selected is based on the production of a known pressure in the detector envelope by controlling the flow of hydrogen gas into and out of the detector volume. A gauge calibration system schematic is shown in Figure 1. The pressure external to the satellite, which is to be measured, is P_0. A calibration is performed in the neighborhood of P_0 by introducing a known pressure increment within the gauge envelope. The pressure increment is produced by applying a temperature pulse to a thermal diffuser located within the gauge enclosure. The temperature pulse increases (exponentially) the gaseous diffusion rate thru the wall of the diffuser, producing a flux of calibrating gas $\dot{Q}$. The resulting gas pressure within the gauge enclosure is

$$P_d = P_0 + \frac{\dot{Q}}{C} , \tag{1}$$

where C is the gas conductance between the diffuser and the exterior. Ionic pumping of the gauge is considered to be negligible compared with the gas conductance to the exterior of the satellite. By regulating the diffuser temperature and thus the flow of calibrating gas, P_d may be varied over a prescribed pressure range.

During the first phase of the program, performance goals were defined for a calibration system applicable to a pressure (or partial pressure) detector on a satellite executing an elliptical orbit. These goals are as follows:

1) System to calibrate a gauge at pressures of 1×10^{-7} Torr and 1×10^{-9} Torr by increasing the pressure within the gauge to 1×10^{-6} Torr and 1×10^{-7} Torr, respectively.

2) The calibrating pulses to have less than a 1% effect in subsequent pressure measurements.

3) The rise-time of the calibration pulse to be less than 3.5 minutes. The pressure then to remain steady at the calibrating level for 10 seconds. The pressure level due to calibrating gas must then decrease to neglible values in less than 15 minutes.

2

Gauge Envelope

Satellite
Surface

P_d

P_O

Gauge

$\dot{Q}$

Conductance C

Space
Environment

Diffuser
Hydrogen Supply
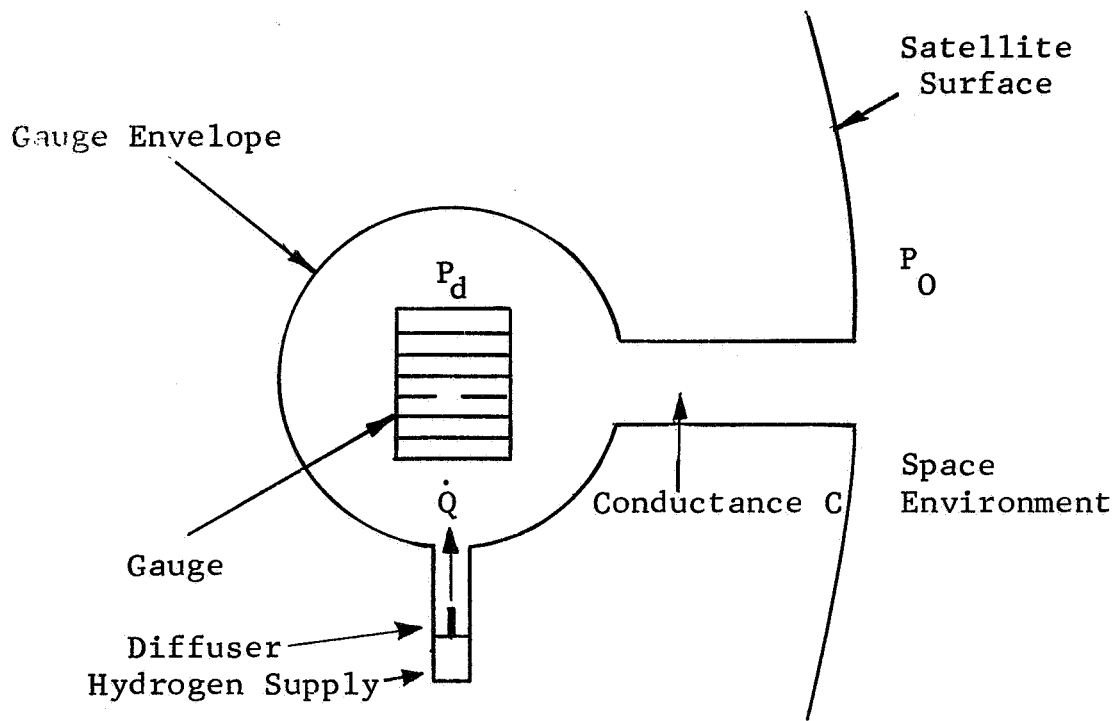
FIGURE I

SCHEMATIC OF SATELLITE CALIBRATION SYSTEM

4) Maximum power consumption of the thermal value
   to be less than 5 watts.

5) Number of calibrations required: 12. One per
   month over a 12-month period.

6) Volume of gas to be carried: less than 100 c.c.

7) Telemetry rate for pressure data: 20-60 samples/
   seconds. Telemetry rate for temperature data:
   20 samples/second.

8) Satellite temperature: -10 to $+50^{\circ}C$.

9) Volume of gauge and conductance to be less than
   330 c.c.

10) Conductance to exterior of satellite to be greater
    than 10 ℓ/second.

11) Time constant of system for pressure variations
    to be less than 0.03 seconds.

12) Roll frequency of satellite: 3 cps.

13) Mass of system to be a minimum.

During phase one, two prototype calibrators, Mark I and
Mark II were designed, constructed, and tested and the results
of those tests used to design and construct Mark III Calibrator.
The work performed in that phase was summarized in a final re-
port issued in November 1965. The objective of this phase of
the program is to experimentally evaluate Mark III Calibrator and
to determine its compatibility with the above performance goals.

Figure 2 shows a detail schematic of Mark III and Figure
3 shows Mark III joined to a Redhead normal magnetron gauge
(NRC 552). In the construction of Mark III only materials suit-
able for operation at high temperatures were used. For example,
all braze joints required were made with gold-nickel braze (M.
P. $950^{\circ}C$), thus allowing high degassing temperatures in order
to obtain improved low pressure performance.

A vacuum jacket was built around the stainless steel tube

Diffuser (304L S.S., .079"O.D., .005"Wall)

Nickel Post

See Detail "A"

.0003" dia. Tungsten Filament (coiled coil)

Ceramic Tubing

Guard Vacuum

.012" Nickel Post

.008" Platinum Clad Tungsten Wire

OFHC Copper

Glass-Kovar Seal

Kovar

Gold-Nickel

Detail "A"

Ceramic Insulator

Vacuum Jacket

Vacuum Jacket Pumping Port

Gold-Nickel Braze

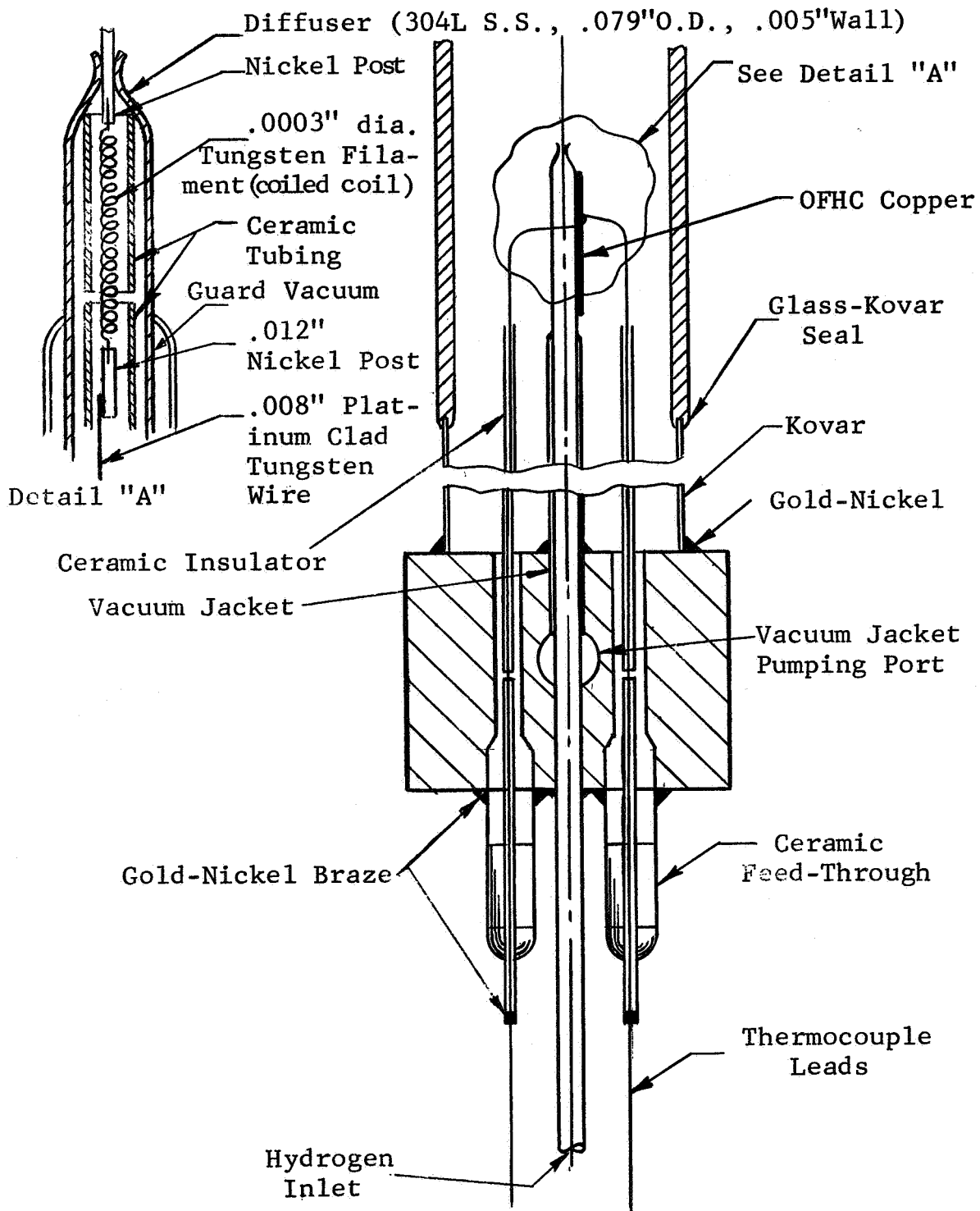Ceramic Feed-Through

Thermocouple Leads

Hydrogen Inlet

FIGURE 2

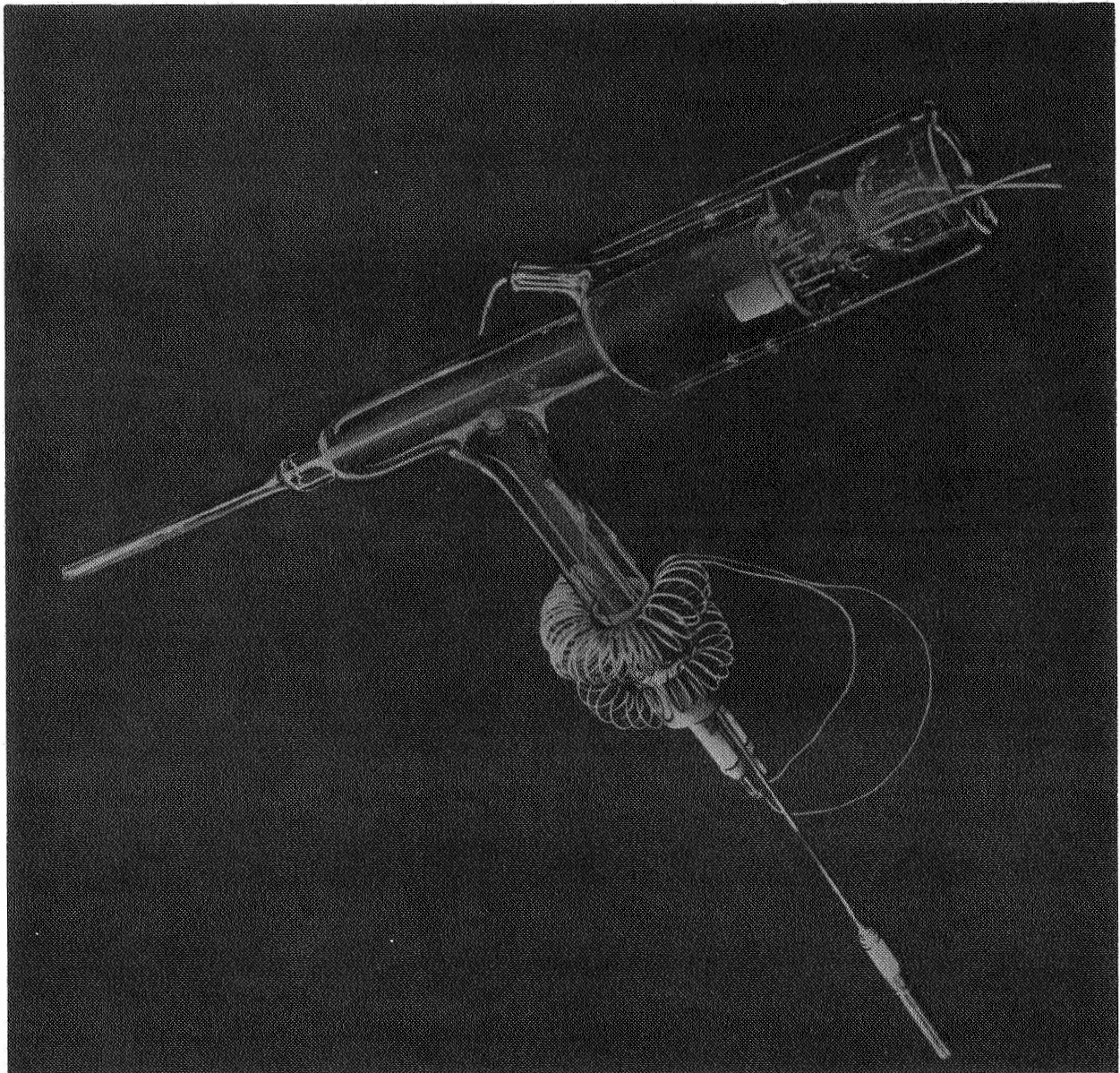SECTIONAL SKETCH OF MARK III CALIBRATOR

5

FIGURE 3

MARK III CALIBRATOR JOINED TO MAGNETRON GAUGE

below the diffuser section to more precisely define the diffusing area and to reduce the thermal isolation of the diffuser section. This was done to improve low pressure performance and increase the rate of cool down and thus the pressure decay rate following a calibration pulse. In addition, a thick OFHC copper plate was brazed to the diffuser section to assure that the diffuser area would be isothermal. The thermocouple was attached directly to the copper plate to provide accurate temperature data during rapid transients. Finally, the normal magnetron gauge was used to measure P_d so that reliable pressure measurements could be extended to the 10^{-12} Torr range.

3. EXPERIMENTAL APPARATUS AND PROCEDURE

The Mark III Calibrator and associated magnetron gauge were joined to an oil diffusion pumped ultra-high vacuum system, having two anti-migration LN_2 cold traps. This system is shown in Figure 4. Figure 5 is a schematic of the system. In Figure 4, a modulated Nottingham gauge is shown joined to the system in place of the reference magnetron gauge. The circular table below the top cold trap is the base of a bakeout oven which was used to degas the top trap, system gauges, high vacuum valve, and Mark III Calibrator. During system bakeout, the lower anti-migration cold trap was filled with LN_2. Prior to starting the 4" diffusion pump, the lower cold trap was heated to 450°C with the 2" diffusion pump operating so as to maintain the system pressure low during bakeout. During the course of the program, the system was degassed at 425°C for five periods greater than 24 hours each and over two weekend periods at 320°C and 380°C.

Data were taken with the system cooled to room temperature (~22°C). Continuous recording on a Honeywell Electronik 17 two-pen recorder was made of the reference magnetron and diffuser magnetron collector currents using Keithley 610R and 410 electrometers. The diffuser copper-constantan thermocouple EMF was measured with a Keithley 148 Nanovoltmeter and continuously recorded with a Moseley 680 autograph recorder. The thermocouple wire was precision grade with a standard error limit of +0.2°C. The temperature was obtained from the National Bureau of Standards thermocouple table.[1] For EMF's greater than the standard range, an extrapolation was made of the table using
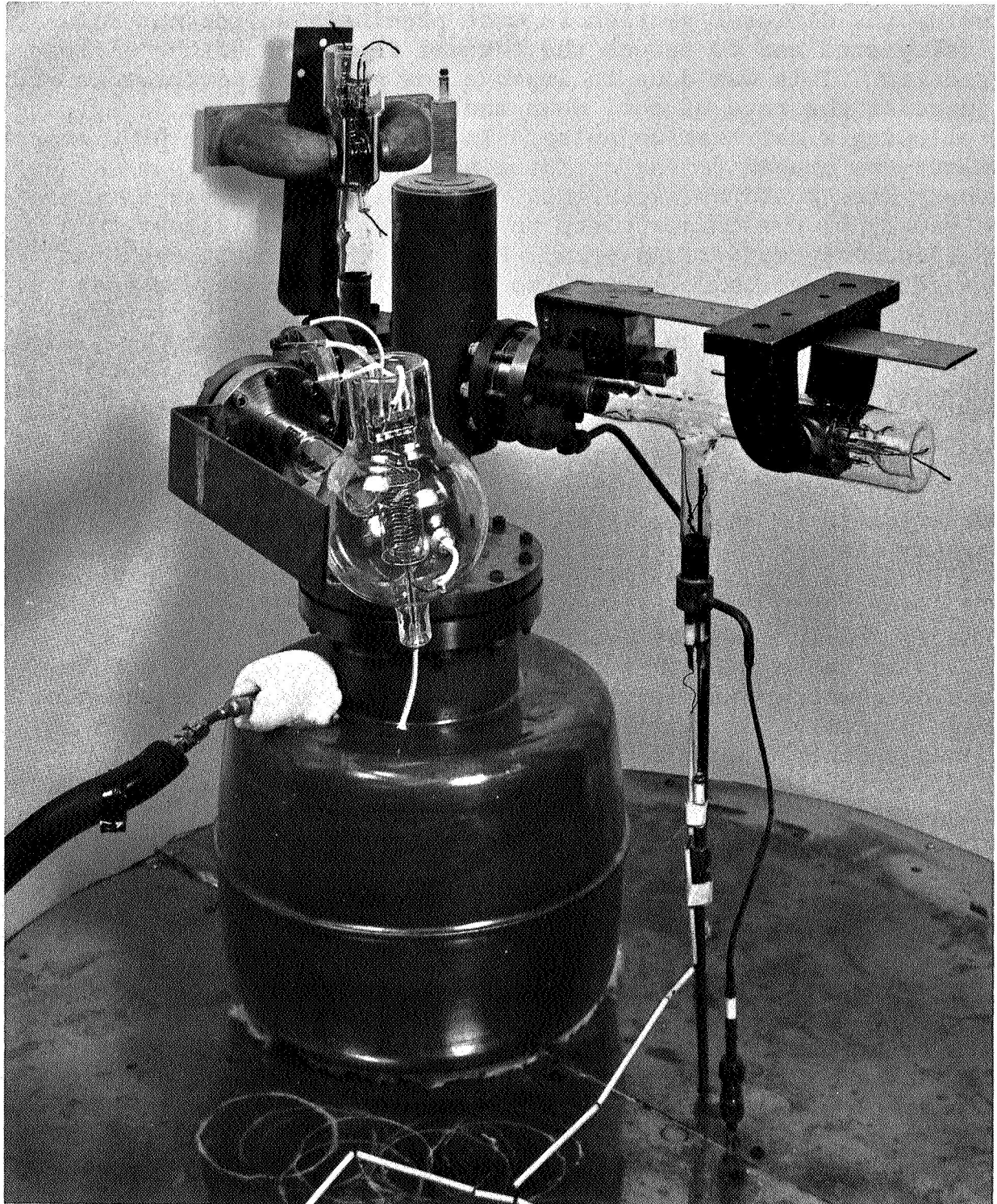
FIGURE 4
MARK III CALIBRATOR AND ASSOCIATED GAUGES
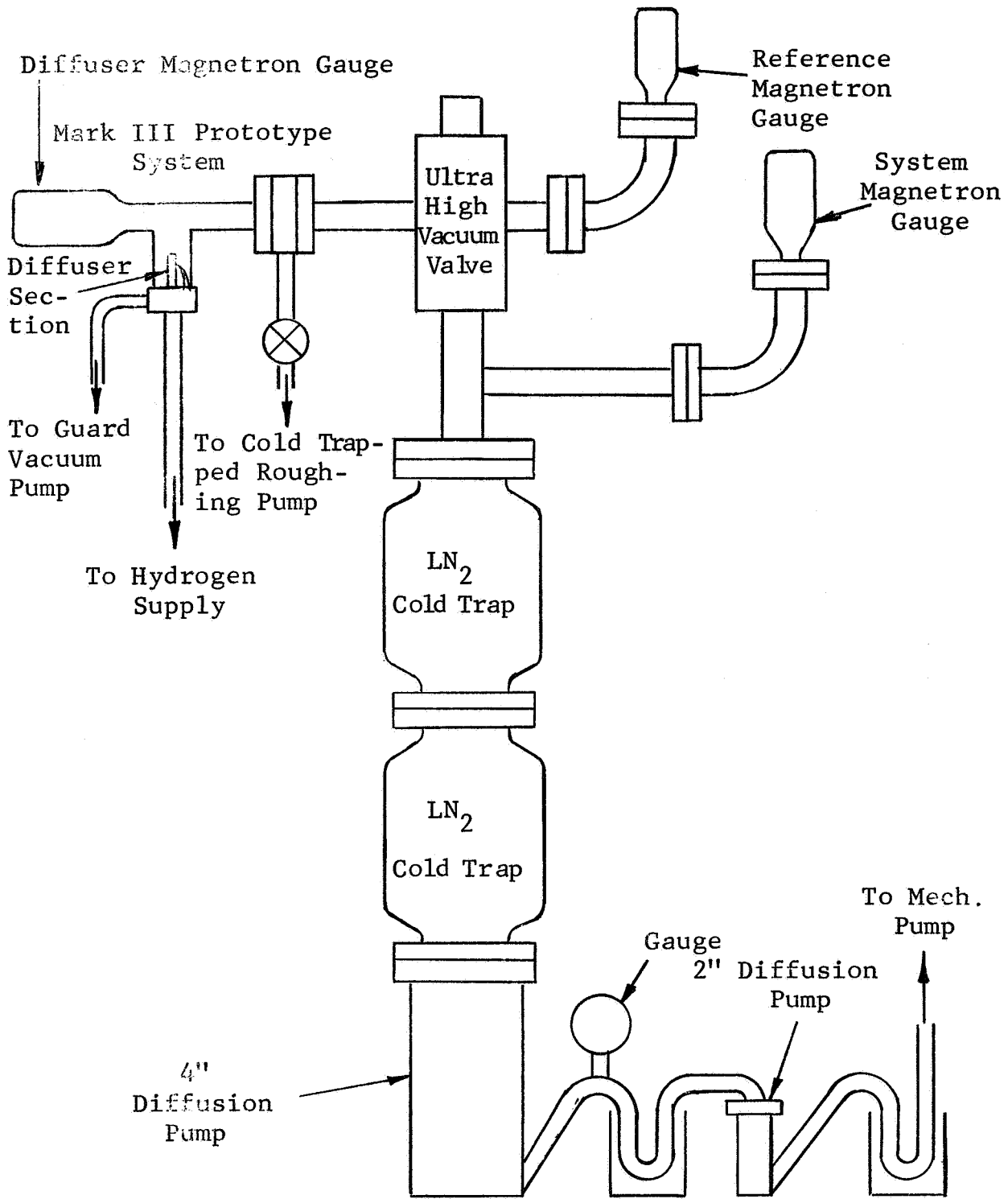ATTACHED TO VACUUM SYSTEM FOR TESTING

FIGURE 5

SCHEMATIC CONFIGURATION OF SYSTEM FOR
MARK III PROTOTYPE PERFORMANCE TESTING

a quadratic fit that agreed extremely well in the 300-400°C range. Heat sink temperature, when obtained, was measured using a thermistor in a Wheatstone bridge circuit. Heat sink temperature was varied by varying the temperature of a massive brass block clamped to the heat sink with brass filings in between. The brass block was in thermal contact with a variable set point constant temperature circulator and was insulated with several layers of aluminized Mylar.

Linde regent grade ultra-pure hydrogen obtained in metal cylinders from J. T. Baker Chemical Company was used. A batch analysis by Linde of the hydrogen used showed the following impurities:

$$H_2O \quad 2 \text{ PPM}$$

$$O_2 \quad 3 \text{ PPM}$$

$$CH_4 \quad 1 \text{ PPM}$$

$$N_2 \quad 1.8 \text{ PPM}$$

The all-metal gas transfer system was evacuated using LN_2 trapped mechanical pumps. The gas pressure was measured with a rotating piston gauge primary pressure standard (CEC type 6-201-0001). The hydrogen gas was then captured by closing a crossover valve aroun, a differential pressure gauge (MKS Baratron Type 77H-1068) which was used to continuously monitor the gas pressure in the Mark III diffuser volume.

Power was supplied to the diffuser heater from a regulated low voltage power supply (ERA model TRO4OM). The current and voltage to the heater were measured with ½% laboratory meters (Weston Model 901). All measurements were made with either 14.6 psi or 29.5 psi ±¼% hydrogen pressure in the diffuser manifold.

The data were obtained over a period of 1½ calendar months, and the measurements were of two distinctly different types as follows:

1)   Steady-state measurements were made of the equilibrium pressure attained in the system after applying a constant voltage to the diffuser heater. The pressure of the system after reaching the steady-state (generally defined as less than ¼ percent

10

variation in measured pressure during a period greater
than several minutes), the temperature of the diffuser,
the voltage and current to the diffuser heater, and
in some cases the heat sink temperature were observed.

2) Transient measurements were made of the quasi-steady-
state pressure obtained by applying a 3 minute heat-
ing pulse at constant applied voltage and then switch-
ing into the circuit for 30 seconds a series resis-
tance of such a magnitude that the diffuser temperature
and thus the system pressure remains constant to within
$\pm 2\%$ for thirty seconds. All the quantities measured
in the steady-state runs, with the exception of the
heat sink temperatures, were also measured in the
pulse runs. In addition, the voltage and current to
the diffuser heater were measured during the plateau
period of the pulse.

The lowest system pressures were attained immediately after
cool down from a bakeout. The lowest pressure measured during
the program was 9×10^{-12} Torr (equivalent N_2) at the system
pressure gauge. It is believed that the system pressure is
limited by the rate of decomposition of the DC 705 oil used in
the diffusion pump since the ultimate pressure was not steady
but was composed of closely spaced random amplitude pulses de-
pendent to some extent on the diffusion pump heater power. The
lowest pressure measured at the reference and diffuser gauges
was 1.5×10^{-11} Torr (equivalent N_2). The magnetron sensitivity
was determined from the data of Feakes, et al[2], for nitrogen
and corrected to hydrogen by using 2.2 A per Torr above 10^{-9} A,
which is the break point below which the NRC 552 becomes non-
linear. Below 10^{-9} A the hydrogen calibration was assumed to
follow the same power law as found by Feakes, et al[2]. Their
data were adjusted for hydrogen by multiplying the current axis
by 0.488 to obtain hydrogen pressure.

4. RESULTS

4.1 Preliminary Experiments

An initial low temperature run was made to determine the
effect of heat sink temperature variation on the calibration

pressure. The heat sink was initially cooled to $257^{O}K$. Upon admitting 14.6 psi of hydrogen to the diffuser no variation in P_d, the pressure in the calibrator magnetron gauge, was found. The temperature of the heat sink was slowly raised to $352^{O}K$. No variation in P_d was noted, even for a temperature of the diffuser as high as $342^{O}K$. It was concluded from the experiment that the time required to set up equilibrium diffusive flow in the stainless steel tube was longer than 10 hours for temperatures near $300^{O}K$.

Reference to the time to set up equilibrium will be made in a manner alalogous to the work of Barrer[3]. For the general case of flow through a plane sheet of thickness ℓ in which the concentration is maintained at a constant C_o on one side and $C_\ell = 0$ on the other, the approach to equilibrium flow is as shown qualitatively in the Q-t plane in Figure 6. The backwards extrapolation of the equilibrium flow rate meets the abscissa at a time τ which is called the lag time and is found to be related to the diffusion constant as follows

$$\tau = \frac{\ell^2}{6D} \tag{2}$$

Actually, the hydrogen concentration at the high pressure surface of the diffuser wall is not constant as the temperature increases. The total hydrogen supply volume is large compared to the internal volume of the diffuser. The volume external to the diffuser remains at room temperature even though the temperature of the gas within the diffuser internal volume may increase by several hundred degrees. Therefore, the pressure throughout the hydrogen supply volume (including the diffuser internal volume) remains substantially at the initial hydrogen charge pressure (generally about 1 atmosphere) independent of diffuser temperature. Thus, the hydrogen density in the diffuser internal volume decreases like T^{-1} as the diffuser temperature increases. The number of hydrogen molecules colliding with unit area of the high pressure surface of the diffuser wall in unit time, therefore, decreases like $T^{-\frac{1}{2}}$. From this effect alone, the hydrogen concentration in the diffuser wall at the high pressure surface must decrease as the temperature increases. However, the hydrogen solubility in stainless steel increases with temperature faster than $T^{\frac{1}{2}}$ (based on solubility data in the literature[4]). Thus, the total effect of temperature is such that
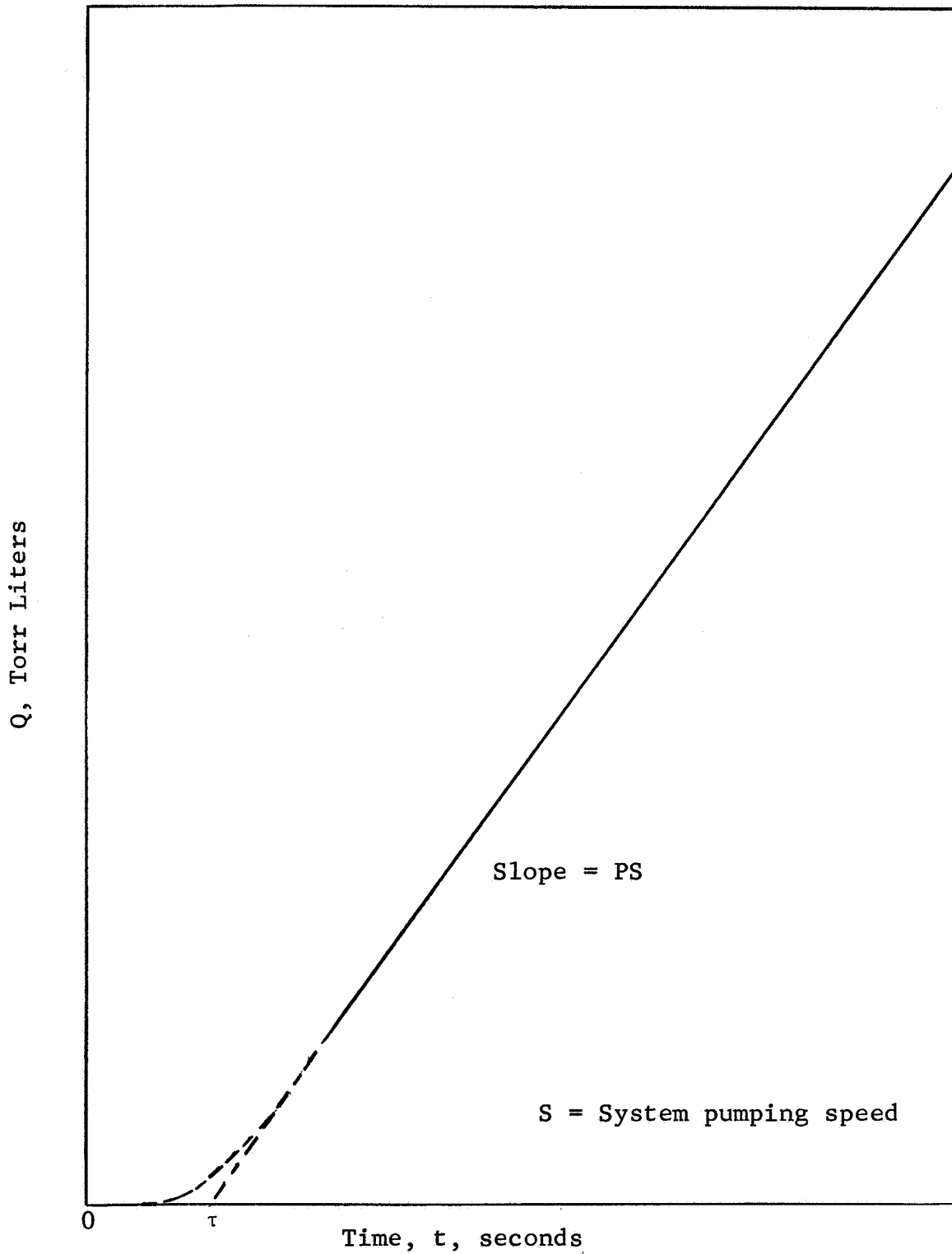
12

FIGURE 6

INITIAL DIFFUSION OF GAS THROUGH A SOLID BODY

the hydrogen concentration in the high pressure surface of
the diffuser increases with temperature.

4.2   Steady-State Diffusion Experiments

To establish an initial hydrogen concentration gradient
within the stainless steel diffuser tube, the sink was kept
near room temperature by convective cooling with room air and
the diffuser was heated by applying power to the heater. No
increase in P_d was observed after 10 minutes of heating at
temperatures up to 450°K. Upon increasing the temperature to
530°K, the first diffusion of gas was noted causing P_d to in-
crease within several minutes time by two orders of magnitude.
It was concluded that the lag time at 520°K was less than 1000
seconds. The diffuser temperature was increased to 550°K to
establish equilibrium hydrogen concentration in the diffuser.

Over a period of several weeks, many separate experiments
were carried out to define the functional form of the steady-
state pressure versus temperature over the range of pressure
from 10^{-12} to 10^{-6} Torr (H_2). The diffuser temperature was
varied over the range 280°K to 770°K. Measurement of temper-
ature at the high end of this range required extrapolation of
the thermocouple EMF table as discussed earlier. Figure 7 is
a plot of log P_d versus 1/T for the data obtained in these ex-
periments. It is noted that there is a large deviation from
linearity of the data in the region of low pressure. A care-
ful look at the data shows that the pressure at which deviation
from linearity occurs depends upon the pressure attained in the
previous diffuser experiments and thus does not act like a
typical background due to outgassing.

In Figure 8, the data for the steady-state experiments is
replotted, but with the initial background of each experiment
substracted. It is seen that the data are grouped closely about
a straight line over the whole range of pressure investigated.
This is the expected behavior for diffusive flow of hydrogen
through the wall of the stainless steel diffuser tube. The
slope of the plot yields the effective activation energy for
the diffusion process.

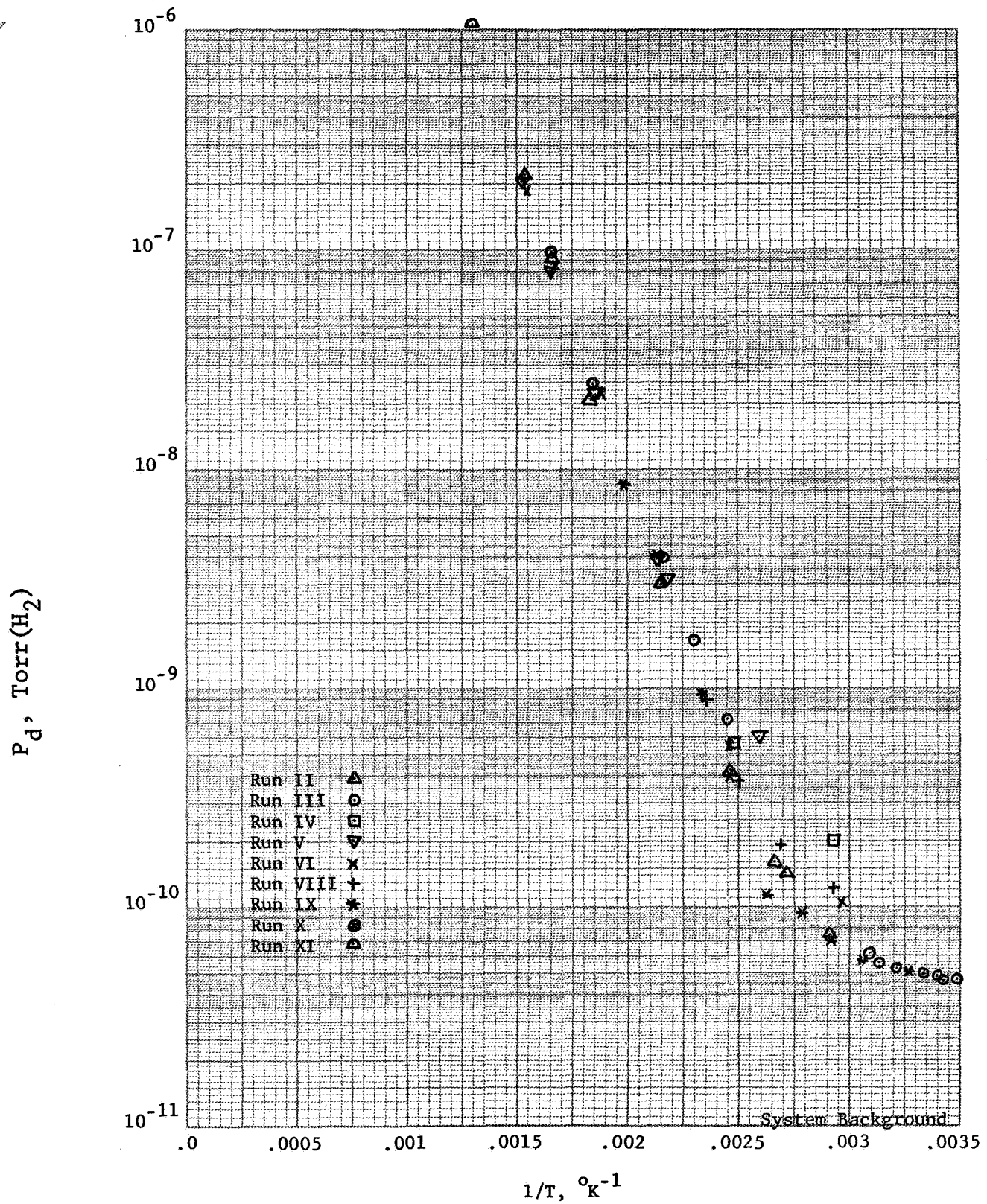The least squares fit to the straight line was calculated

14

FIGURE 7

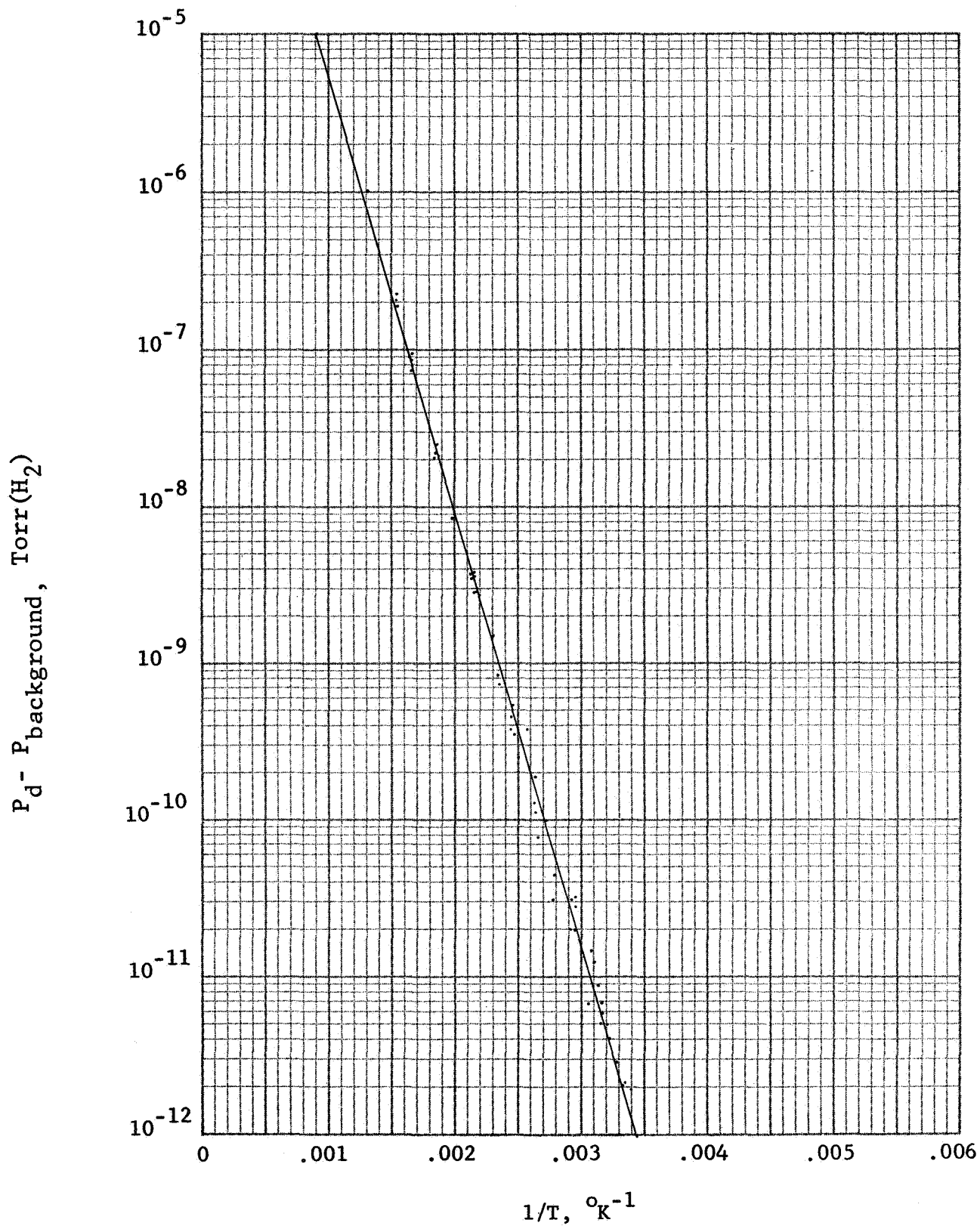DIFFUSER GAUGE PRESSURE FOR STEADY STATE EXPERIMENTS

15

FIGURE 8

STEADY STATE DIFFUSER GAUGE PRESSURE, CORRECTED FOR BACKGROUND

16

and is shown on Figure 8. The relative standard error of estimate for the least squares fit is 1.3% to all the data. This low error indicates, among other things, that the effective diffusion area is constant, a fact influenced by the improved design of the Mark III diffuser shorting bar and the use of a guard vacuum around the hydrogen supply tube.

In order to test for curvature, a second order least squares fit was tried but this procedure did not lower the standard error of estimate. This is not surprising for there is no physical basis for expecting the quadratic term. However, by determining the least squares fit to a straight line for different parts of the whole pressure range, there was found to be a systematic increase in slope and decrease in standard error of estimate as more of the lower pressure points were neglected. For example, considering only the 10^{-8} to 10^{-6} Torr (H_2) points, the slope is 9% higher than for the 10^{-12} to 10^{-6} points. This variation is summarized in Table I. It may also be seen that the relative standard error of estimate of the least squares fit decreases as the lower pressure data is dropped out. There are several reasons for this behavior. First, as the temperature of the diffuser is increased there is a tendency for it to become more isothermal and thus the parts of the tube beyond the copper shorting strip can contribute comparatively more to the flow than at lower temperatures. Second, as will be shown later, in the lower part of the temperature range, the hydrogen concentration within the diffuser wall is higher than the equilibrium concentration corresponding to that range. Third, as discussed later in section 4.7, the hydrogen flux through the diffuser was observed to depend on hydrogen supply pressure more strongly than the ½ power. This implies that at high temperature a molecular hydrogen flux component becomes observable (presumably due to molecular hydrogen flow along grain boundaries). Thus, the total flux observed in the calibrator at high temperatures may be the sum of the atomic hydrogen diffusion through the metal and molecular hydrogen diffusion along grain boundaries. Finally, as has already been pointed out, the hydrogen concentration in the high pressure surface of the diffuser increases with temperature.

TABLE I

STEADY-STATE EXPERIMENT SUMMARY

Pressure Range, Torr(H_2)	A	B, ^{o}K	Error, percent
10^{-12} - 10^{-6}	-2.512	-2764	1.3%
10^{-11} - 10^{-6}	-2.460	-2789	1.2%
10^{-10} - 10^{-6}	-2.315	-2863	1.0%
10^{-9} - 10^{-6}	-2.298	-2870	0.6%
10^{-8} - 10^{-6}	-2.020	-3040	0.4%

where A and B are the constants in the least squares fit of the data to

$$\log(P_d - P_{background}) = A + \frac{B}{T} \, ,$$

and the error given is the relative standard error of estimate for the least squares fit.

18

The lowest pressure points were measured in an experiment to determine the effect of heat sink temperature variation (to simulate the variations in temperature of a spacecraft). This run was made after a large concentration of hydrogen had been established in the diffuser. The diffuser heater was not activated but rather the diffuser was heated by conduction from the heat sink. The fact that these points fit so well to the straight line for the higher temperatures obtained by using the diffuser heater indicates the success, in the Mark III design, of the copper shorting bar in maintaining the diffuser iso-thermal and the diffuser guard vacuum in accurately defining the diffusing area.

4.3 Diffusion Constant and Lag Time

Some steady diffusion points were obtained for a set of equilibrium temperatures such that each temperature was less than the previous temperature. These data contained evidence that the hydrogen concentration in the diffuser did not arrive at its new equilibrium concentration within the same time interval required to establish a new equilibrium temperature. For example, after a constant pressure experiment at a diffuser temperature of $769^{\circ}K$, the temperature was lowered to $569^{\circ}K$ and was stable after 11 minutes. However, the pressure continued to decrease for an additional 10 minutes to about 95% of its value at the time of reaching temperature equilibrium. It, thus, becomes obvious that knowledge of the effective diffusion lag time, τ, as a function of temperature is required.

To obtain τ, a step change in pressure was generated on the high pressure side of the diffuser and the variation in diffusion rate with time was observed. The effect of this change in pressure on a Q - t plot is shown in Figure 9. In analogy with the earlier definition of τ, the lag time derived from such an experiment for a change in low side pressure from P_0 to P_F is indicated in Figure 9. By analytical calculus it may be seen that τ is given by

Q, Torr Liters
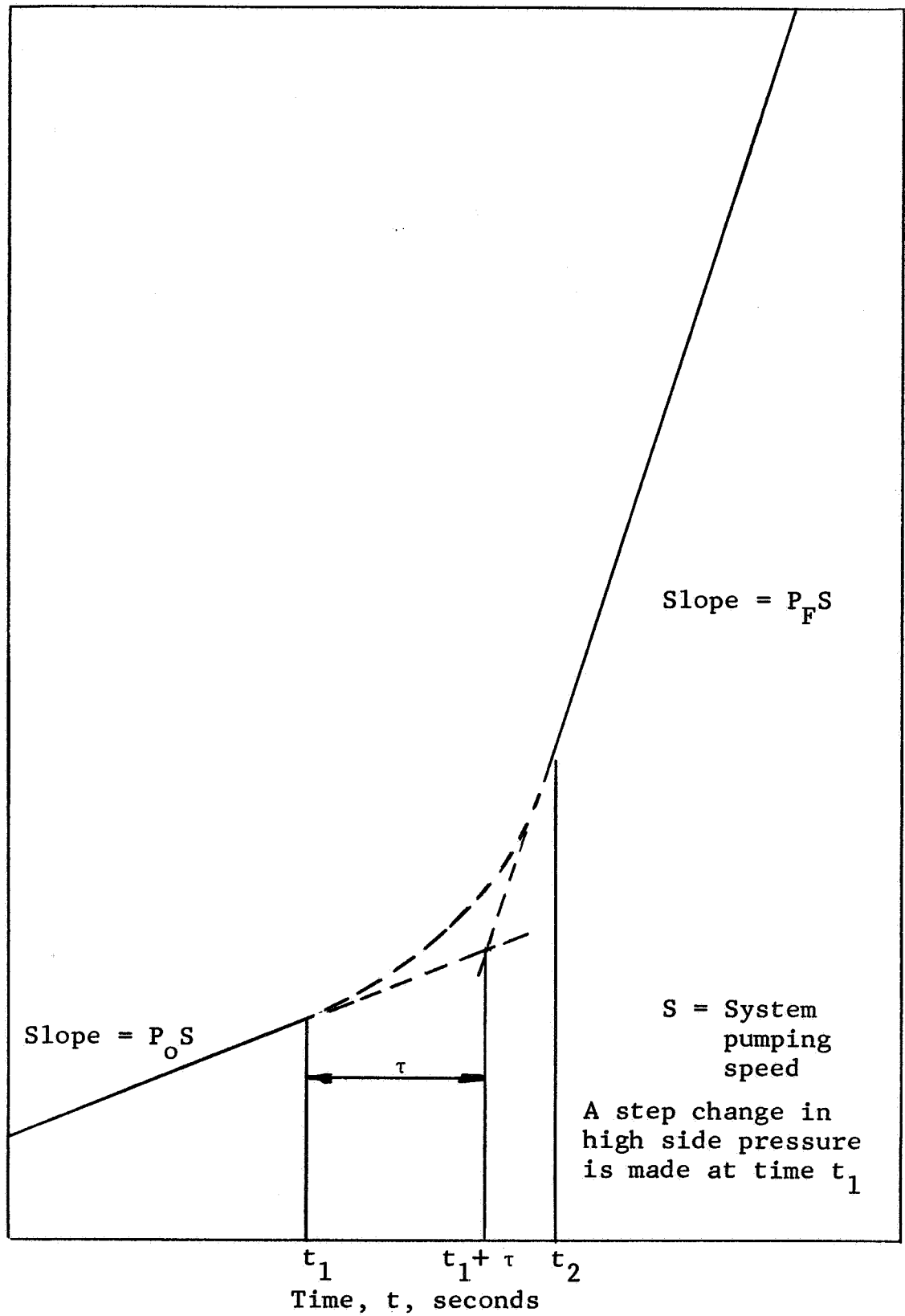
Slope = $P_F S$

Slope = $P_O S$

τ

S = System
pumping
speed

A step change in
high side pressure
is made at time t_1

t_1 $t_1 + \tau$ t_2

Time, t, seconds

FIGURE 9

CHANGE OF FLOW RATE OF GAS THROUGH A SOLID BODY

20

$$\tau(T) = \frac{\int_{t_1}^{t_2} P \, dt - P_F(t_2 - t_1)}{P_0 - P_F} \qquad (3)$$

The lag time, τ, was determined for 5 temperatures and the results are given on a semi-log plot versus $1/T$ in Figure 10. An attempt to determine τ at 500°K was unsuccessful due to the excessive time involved although a lower limit of 1000 seconds was obtained for that temperature. The least squares fit to the data is also plotted. It may be seen that τ becomes long compared with the usual cooldown time of hundreds of seconds at the comparatively high temperature of 580°K and that for room temperature τ is about 10^7 seconds.

The effective diffusion coefficient D^*, for $P_{H_2} = 14.6$ psi was obtained from equation (2) and the lag time, τ. The results are shown in Figure 11 along with data reported by Flint[4] and by Lewin[5]. In addition, the effective diffusion coefficient was obtained from

$$D^* = 1.32 \frac{S_p(H_2) P_d \, \ell}{A} \frac{cm^2}{sec} , \qquad (4)$$

where P_d is the pressure measured in the steady-state runs, $S_p(H_2)$ is the effective pumping speed for hydrogen at the diffuser, ℓ is the thickness of the diffuser, and A is its area. The pumping speed of the system was determined for argon in an auxiliary experiment with a porous Vycor plug whose conductance is accurately known. Using free molecular flow theory S_p for hydrogen was calculated to be 24 liters/second. The value of D^* thus determined is also plotted in Figure 11 where close agreement is seen with the least squares fit to the points obtained from the pressure change technique.

4.4 Thermal Pulse Diffusion Experiments

Pulses of hydrogen gas with flat tops up to 30 seconds in duration were generated, starting from various initial diffuser temperatures. Background was subtracted from the pressure reached at the plateau similar to the method used in reduction
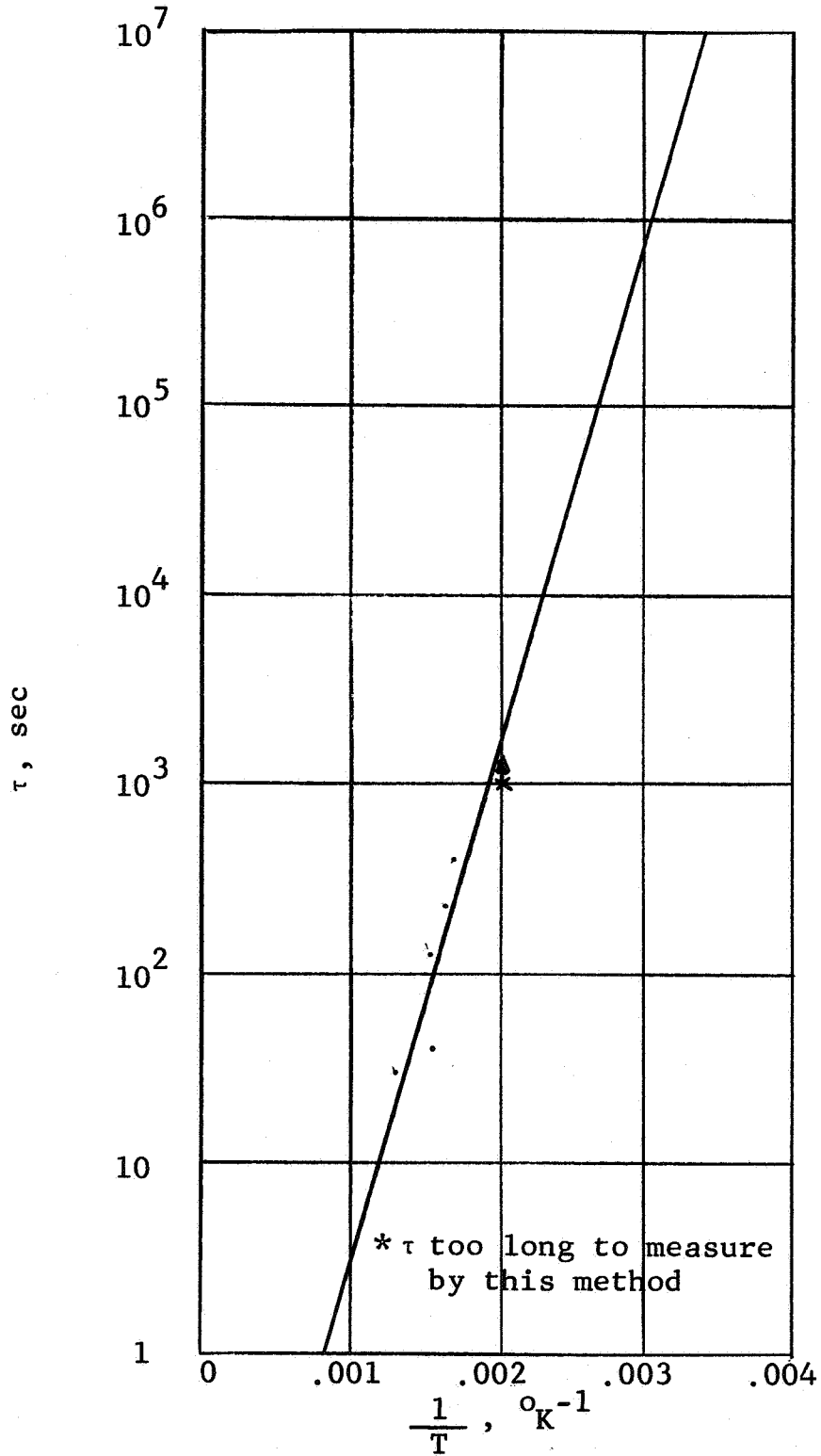
FIGURE 10

EFFECTIVE LAG TIME FOR MARK III DIFFUSER

22

D*, cm²/sec — axis label: D^*, cm^2/sec

10^{-6}

10^{-7}

10^{-8}

⊙ From eqns. 2 & 3
⊡ From eqn 4
✕ Lewin (1966)
+ Flint

$P_o = 14.6$ psi

.001   .002   .003

$\frac{1}{T}$, $^oK^{-1}$
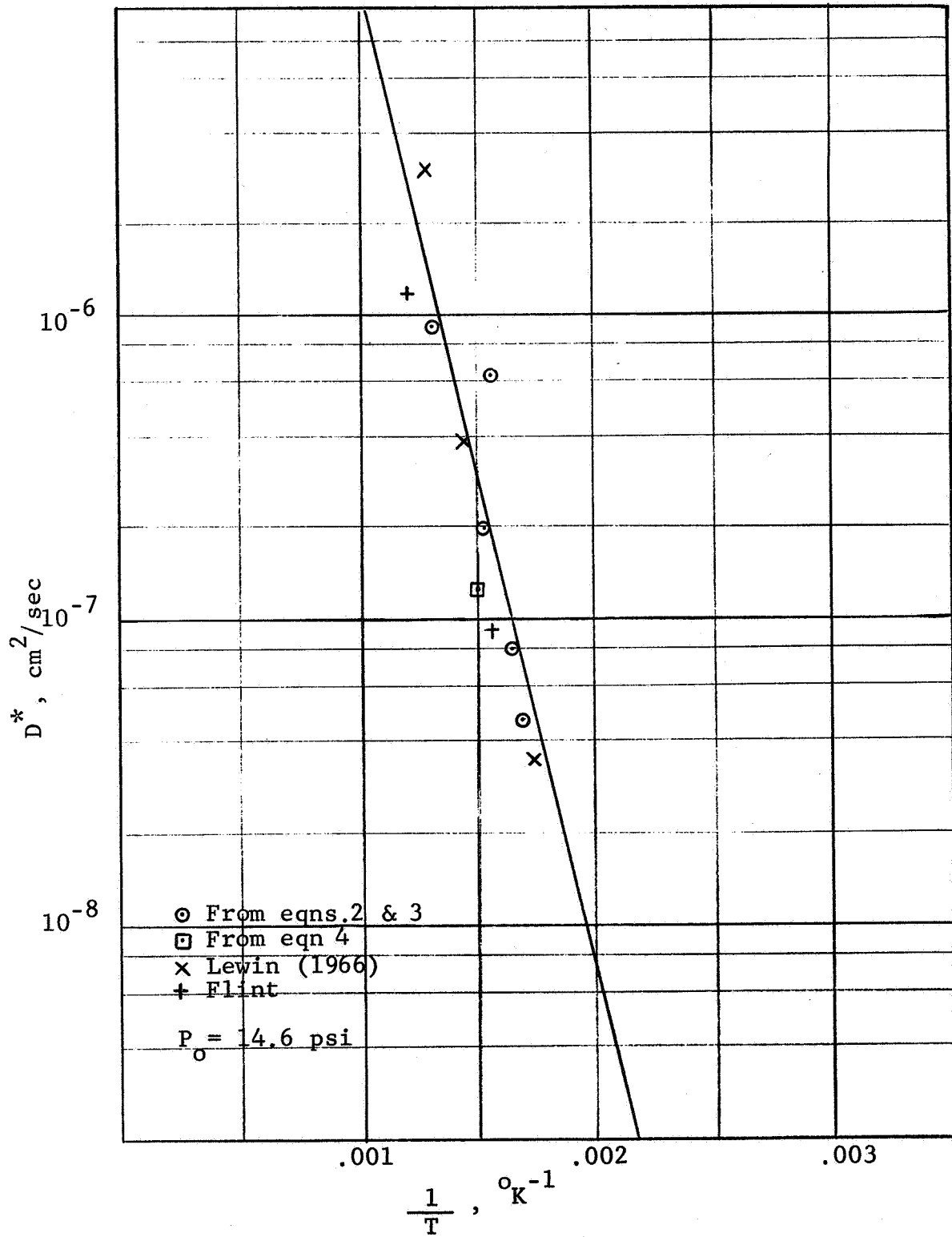
FIGURE 11

EFFECTIVE DIFFUSION COEFFICIENT FOR MARK III DIFFUSER

23

of the steady-state data. Table II summarizes the average value of pertinent parameters for each sub-group of pulses having the same peak temperature. These data were taken over a period of more than a week at various pulse amplitudes and initial temperatures. Only 10 seconds of the plateau were considered in that summary, the pressure constancy over the interval being better than $\pm 1\%$ in general. Figure 12 is a plot of the logarithm of $(P_{plateau} - P_{initial})$ versus $1/T$ for the average values above, also, the least squares fit to a straight line is plotted. The least squares slope is seen to differ from that of the steady-state points for the same pressure range by less than 6%. Some variation would be expected since it was found in the steady-state experiments that temperature equilibrium was not reached in the three minutes used in the pulse runs but rather took up to 25 minutes in some cases. In addition, the number of steady-state high pressure points is small (one point above 3×10^{-7} Torr (H_2)) and, therefore, the high pressure data is less reliable. For example, leaving out the point at 10^{-6} Torr causes the least squares slope to change from -3045 to -2929. The latter slope is within 2% of the steady-state slope for points in the same pressure range.

In order to test the effect of initial temperature on the data, all runs with a plateau temperature in the vicinity of 515°K were corrected to 515°K, using the least squares fit for the pulse runs. Figure 13 shows a plot of $(P_{plateau} - P_{initial})$ for 515°K versus initial temperature. It is seen that the effect of initial temperature is negligible if the background subtraction scheme is followed.

4.5 Pressure Decay Following a Calibration Pulse

It has already been shown that the diffusion time lag, τ, is short at high temperatures. It, therefore, is anticipated that the pressure decay rate following a calibration pulse would be a function of the diffuser temperature decay rate only (at least for high to moderate diffuser temperatures). However, it is found experimentally that the observed pressure decay rate is slower than that calculated from the observed temperature decay rate. Thus, the hydrogen pressure in the calibrator is higher than that corresponding to steady-state diffusion at the instantaneous temperature of the diffuser during cooldown.
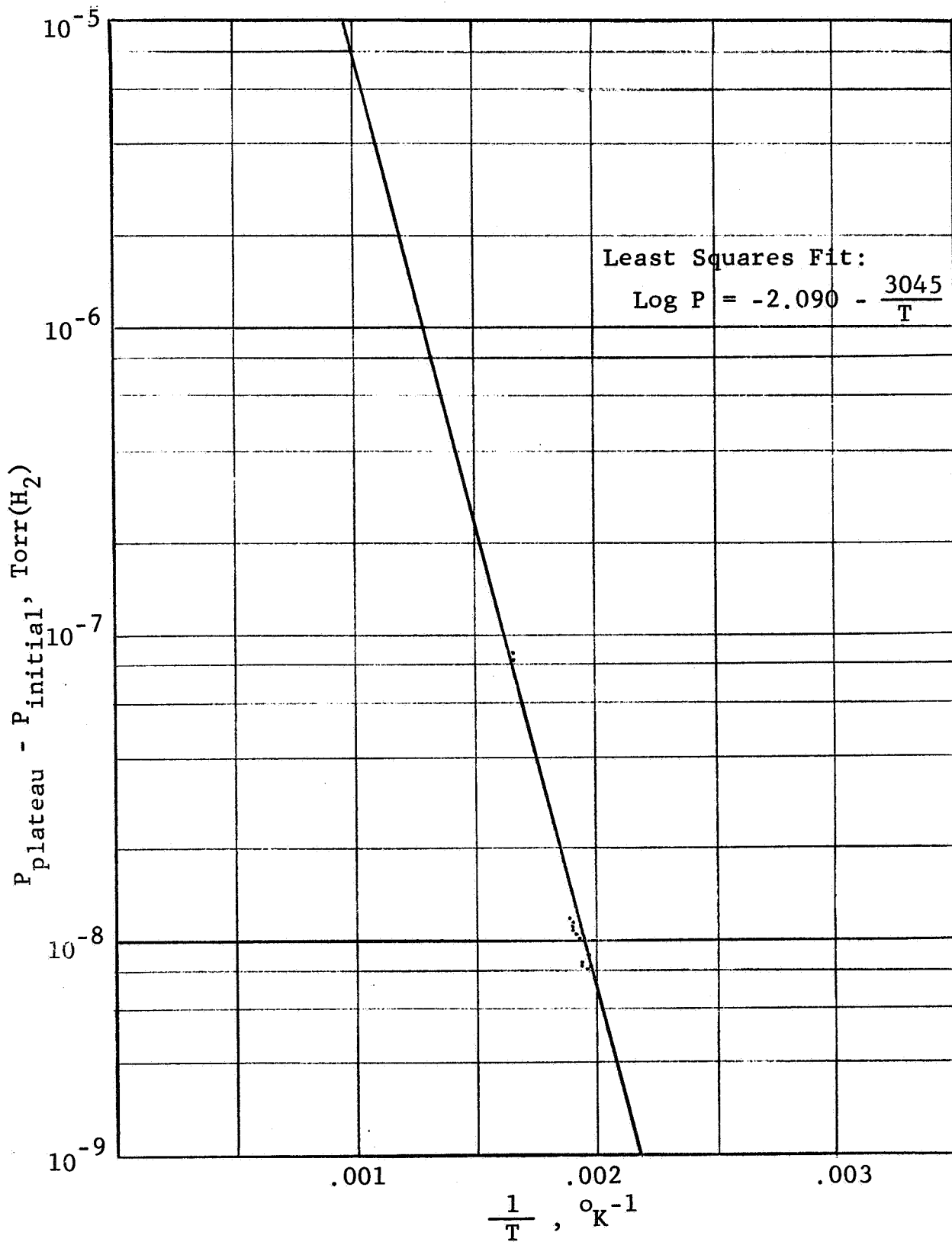
24

Least Squares Fit:

$$\text{Log P} = -2.090 - \frac{3045}{T}$$

FIGURE 12

PULSE PLATEAU PRESSURE, CORRECTED FOR BACKGROUND

TABLE II

SUMMARY OF THREE MINUTE PULSES WITH TEN SECOND PLATEAUS

Pulse Series No.	N	T_i, °K	T_p, °K	$P_p - P_i$, Torr	E, %	V, V	W_{max}, W	R, Ohm	I_p, A
1	8	352	522	1.07×10^{-8}	4.4	7.60	1.98	3.6	.166
2	2	352	521	1.03×10^{-8}	0	7.60	1.91	3.6	.166
3	3	352	526	1.10×10^{-8}	0.5	7.60	1.94	3.6	.166
4	3	352	512	0.92×10^{-8}	2.3	7.50	1.84	3.6	.168
5	4	381	525	1.16×10^{-8}	0.7	7.60	1.98	3.6	.165
6	2	381	525	1.15×10^{-8}	0	7.60	1.79	3.6	.165
7	2	381	529	1.22×10^{-8}	0	7.60	1.67	3.6	.166
8	4	323	606	8.58×10^{-8}	0.5	10.90	3.00	3.0	.200
9	4	323	433	1.00×10^{-9}	0	5.45	1.09	5.5	.140
10	3	323	436	1.00×10^{-9}	0.6	5.40	1.12	4.5	.142
11	3	323	606	8.83×10^{-8}	0.6	11.0	3.85	3.0	.200
12	3	323	777	1.17×10^{-6}	3.2	19.0	10.64	2.2	.254
13	2	294	512	8.19×10^{-9}	0	7.60	2.28	3.6	.170
14	1	297	511	8.40×10^{-9}	-	7.60	2.22	3.6	.185
15	1	297	517	8.65×10^{-9}	-	7.60	2.09	3.6	-

where,

N = Number of data points considered

T_i = Initial temperature of diffuser

T_p = Diffuser temperature during pulse plateau

P_i = Initial pressure in diffuser magnetron

P_p = Pressure in diffuser magnetron during pulse plateau

E = Standard error in $(P_p - P_i)$ for pulse series

V = Voltage applied to system

W_{max} = Maximum measured power dissipation

I_p = Current through diffuser during pulse plateau

Note: W_{max} was the power dissipation observed seconds after the voltage was applied. The initial power drawn with the filament cold was slightly higher.
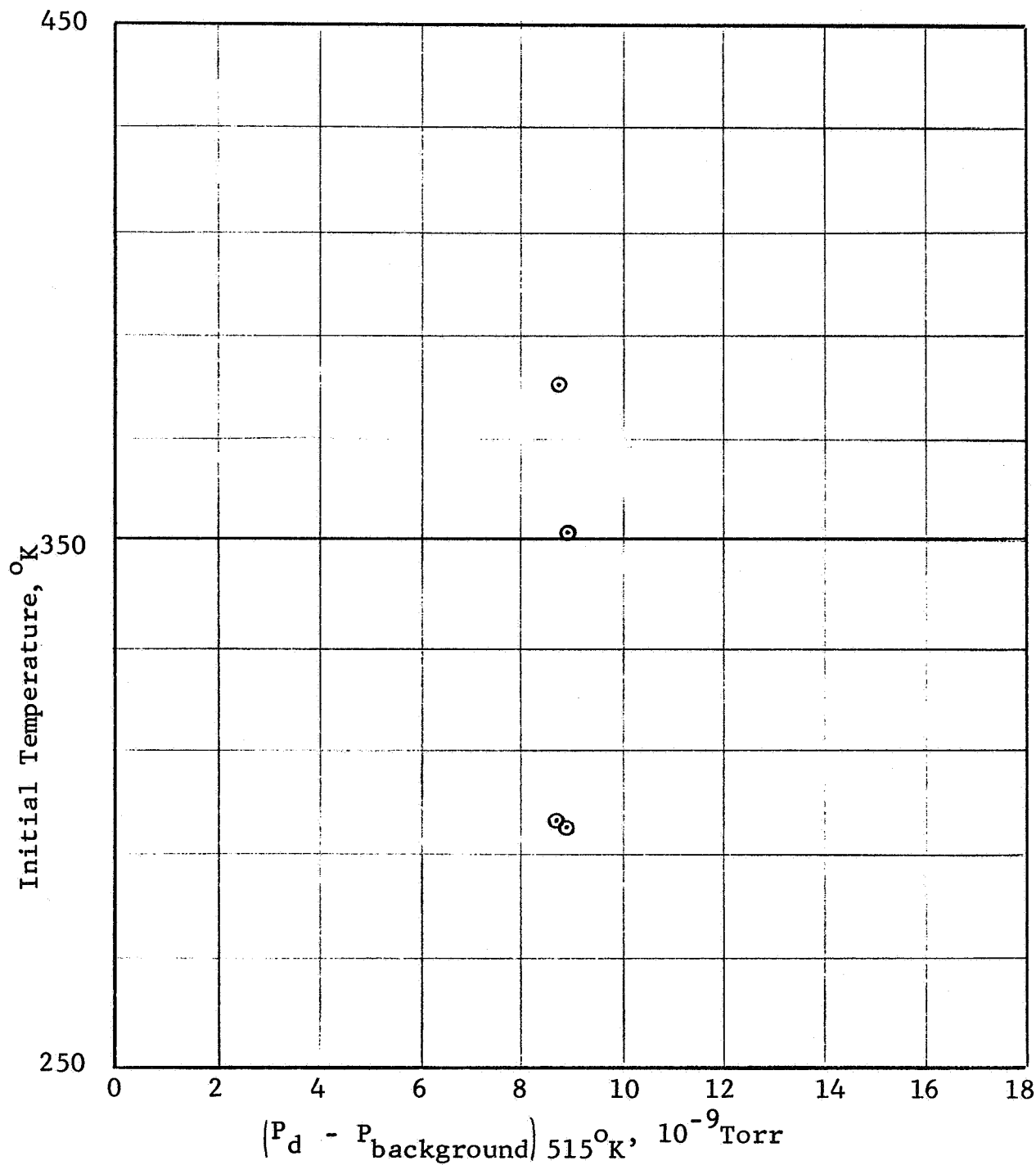
FIGURE 13

EFFECT OF INITIAL TEMPERATURE ON PULSE EXPERIMENTS

In addition to hydrogen adsorption on the surfaces of the electrodes and vacuum enclosure, there are at least two other possible causes of this behavior. First, the hydrogen concentration within the diffuser wall at any instant may be that corresponding to a higher temperature if relaxation of the concentration distribution is a slower process than cooldown (this must happen if the diffuser temperature is sufficiently low). The solubility of hydrogen in stainless steel increases with temperature. The hydrogen concentration distribution corresponding to some higher temperature may be temporarily "frozen-in" during rapid cooldown of the diffuser. Thus, the hydrogen concentration at the vacuum surface of the diffuser would always be higher during cooldown than an equilibrium concentration corresponding to the instantaneous diffuser temperatures. Therefore, the rate at which gas could be desorbed from the vacuum surface would be higher than that corresponding to the steady-state diffusion process at the instantaneous temperature. If recombination to form molecular hydrogen on the vacuum surface is the rate limiting step in the total permeation process, the "frozen-in" nonequilibrium concentration suggested above would probably not be observable. Based on the assumption that the hydrogen concentration becomes "frozen" at about $700^{\circ}K$, (a conservative assumption based on the data in Figure 10), quantitative estimates of the total number of hydrogen atoms in or near the surface of the diffuser which would be available for desorption into the vacuum can account for only a small fraction of the total number of hydrogen molecules observed in the calibrator after the diffuser heater power was turned off, obtained from the time integral of the observed pressure and known conductance to the pumping system.

The second possible cause of the observed reduction in pressure decay rate following a calibration pulse, may be hydrogen liberated by the magnetron gauge. During the calibration pulse about 2% of the total diffuser flux is pumped by the magnetron gauge. - After the diffuser flux is turned off and the pressure in the calibrator begins to decay, the hydrogen ion current to the magnetron cathode decreases. However, the quantity of hydrogen buried in the cathode corresponds to a higher ion incidence rate. This gas must continue to diffuse out of the cathode yielding an apparent hydrogen source until the quantity of gas remaining in the cathode is again in equilibrium with the (lower) ion current. It is not obvious how much time this recovery process requires. Since the cathode is at room temperature the unaided diffusion process would be slow. However,

the cathode is continually bombarded with energetic ions
which produce considerable disturbances on an atomic scale
(temperature spikes) and assist the liberation of hydrogen
from the cathode.

It is, of course, possible that a substantial fraction
of the hydrogen observed in the calibrator after the diffuser
heater power is turned off comes from hydrogen desorption from
the surface within the calibrator where it had been adsorbed
during the high pressure part of the calibration pulse.

Several experiments were conducted to determine the act-
ual source of hydrogen which produced the apparent reduction
in pressure decay rate after a calibration pulse. The dif-
fuser temperature was maintained at $501^{O}K$ for a time compar-
able with the lag time τ at $501^{O}K$ such that equilibrium con-
centration was established in the diffuser wall. After the
diffuser heater power was turned off the pressure and diffuser
temperature were measured as a function of time. The observed
pressure is plotted in Figure 14, along with the pressure cal-
culated for steady-state diffusion from the observed instan-
taneous temperature. The difference between the observed
pressure time history and that calculated from the instantan-
eous diffuser temperature could result from either desorption
or re-emission of hydrogen pumped ionically. From these re-
sults, it is not possible to determine the location of the
gas source.

In another experiment the diffuser temperature was main-
tained at $436^{O}K$ for an interval which was less than 2% of τ
at $436^{O}K$. After the heater power was turned off the pressure
and diffuser temperature were recorded as a function of time.
Figure 15 presents the observed pressure and the pressure cal-
culated from steady-state diffusion for the observed instan-
taneous diffuser temperature. It may be seen that the differ-
ence between the two curves is substantially less than in Figure
14. It is not possible to give an unambiguous explanation for
the closer agreement between the two curves since maintaining
peak diffuser temperature for a short period compared to τ
would prevent the establishment of equilibrium concentration
at $436^{O}K$ and also maintaining peak pressure for a short period
would reduce the number of ions that could be buried in the
magnetron cathode, and at the same time, reduce the total num-
ber of hydrogen molecules adsorbed on the surfaces of the cal-
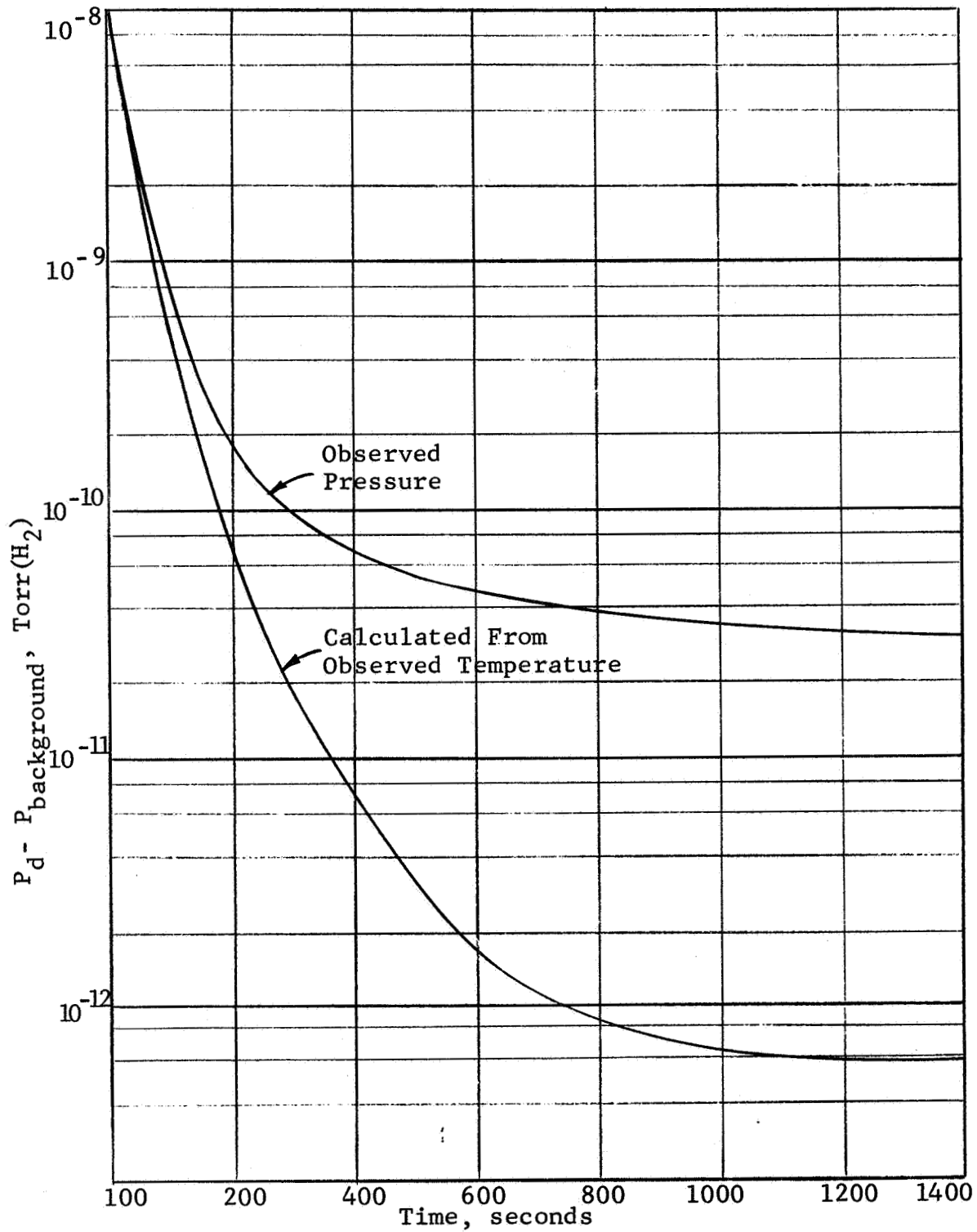ibrator.

30

FIGURE 14

OBSERVED AND CALCULATED PRESSURE DECAY FOR MARK III,
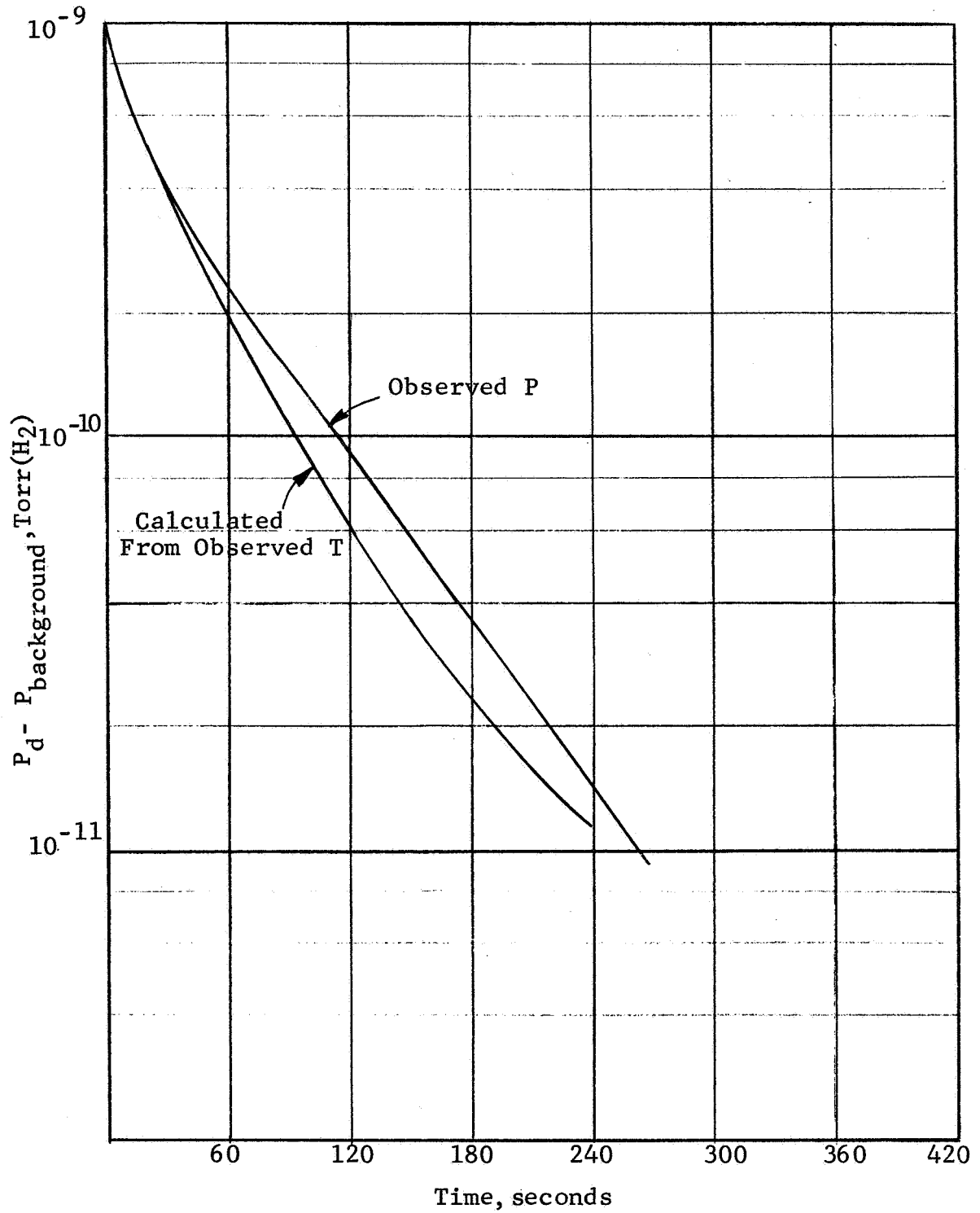COOLED RAPIDLY FROM EQUILIBRIUM AT HIGH TEMPERATURE

31

FIGURE 15

OBSERVED AND CALCULATED PRESSURE DECAY FOR MARK III,
COOLED RAPIDLY FROM NON-EQUILIBRIUM AT HIGH TEMPERATURES

32

The importance of this effect may be appreciated from the following experimental results. The diffuser was heated to 615°K corresponding to $P_d = 2 \times 10^{-7}$ Torr (H_2) and equilibrium hydrogen concentration distribution was established. Heater power was removed and after cooldown the diffuser maintained at 295°K for 2.5 days. This period is short compared to the time lag period at 295°K which may be determined by extrapolating the measured time lag data given in Figure 10 to yield $\tau = 116$ days. The observed pressure after the 2.5 day decay period was 3×10^{-11} Torr, which corresponds to the steady-state diffusion rate for a diffuser temperature of 345°K, if there were no other sources of hydrogen.

4.6 Three Level Pulse Experiments

The practicability of producing calibration pulses in the neighborhood of 10^{-9}, 10^{-8}, and 10^{-7} Torr (H_2) all with a single insertion resistance and fixed power supply voltage by varying the heating period prior to resistor insertion was investigated. The voltage was chosen such that the time required to reach $\sim 10^{-7}$ Torr was less than 3 minutes. The value of the resistor inserted in series with the diffuser heater was chosen such that the peak pressure remained constant within 1.0% for 30 seconds for a pulse height of $\sim 10^{-8}$ Torr (H_2). The results are shown in Figure 16. It may be seen that the peak heights of the high and low pressure pulses do not remain constant to better than $\pm 14\%$ and $\pm 23\%$ respectively.

From these results, it is concluded that the power dissipated in the diffuser heater must be different for each different height calibration pulse. This may be most efficiently accomplished by providing a number of resistors, one tailored to satisfy the dissapation required in the diffuser heater to maintain constant temperature for each calibration pulse height desired.

4.7 Diffusive Flow Dependence on Pressure

The flux for a diatomic gas which reacts with the surface and diffuses through a solid as atoms, recombining to desorb into the vacuum as molecules is given by

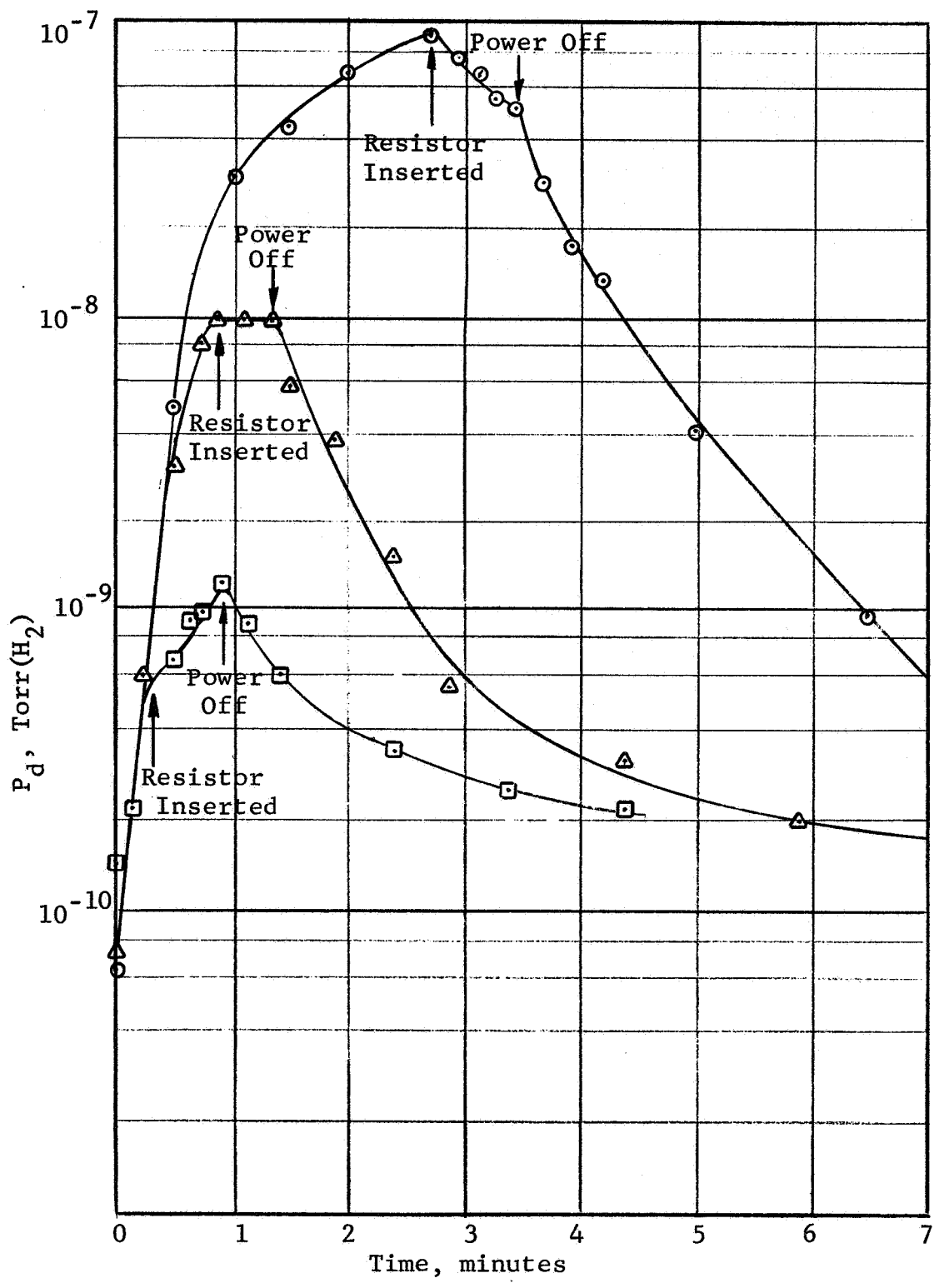$$\dot{Q} = \frac{S(T)D(T)A}{\ell} \; P_h^{\frac{1}{2}} \; \exp(-E/RT), \qquad (5)$$

33

FIGURE 16

THREE LEVEL PULSE

where, $S(T)$ is the gas solubility in the solid, $D(T)$ is the diffusion coefficient, A is the area of the solid thru which the gas is diffusing, ℓ is the length of the solid, P_h is the high side pressure, and E is the activation energy for the diffusion process.

This is considered the flow mechanism in Mark III Calibrator. The pressure on the vacuum side of the diffuser P_d, is related to this flow rate by

$$\dot{Q} = P_d S_p \; , \qquad\qquad (6)$$

where, S_p is the effecting pumping speed of the system, including the effects of ionic pumping by the gauge. Thus, if the high side pressure P_h is changed at constant temperature, it is expected that

$$\frac{P_{d_i}}{P_{d_f}} = \left(\frac{P_{h_i}}{P_{h_f}} \right)^{\frac{1}{2}} \qquad\qquad (7)$$

where, i refers to initial and f to final pressures, respectively. This relation has been tested experimentally and the results are given in Table III. It may be seen that deviations from monatomic diffusion increase with temperature (except for the point at 651°K which has a relatively small deviation). This implies that a small fraction of the hydrogen is diffusing as molecular hydrogen. The deviation from atomic diffusion appears to increase exponentially with temperature.

4.8 Activation Energy for Diffusion

The activation energy in the diffusion process may be obtained from the slope of the Arrenius plots such as Figures 7, 8, or 11. If only the data above 4×10^{-10} Torr (H_2) is considered, in order to leave out the effect of the "background" then the average slope from these three figures is found to be

$$\frac{E}{k} = -6540 \pm 50 \text{ Degrees,}$$

TABLE III

COMPARISON OF OBSERVED P_d WITH DIFFUSION THEORY
FOR MARK III CALIBRATOR

P_{h_i}, psi	P_{h_f}, psi	Temp, ^oK	$\dfrac{P_{d_i}}{P_{d_f}}$	Deviation from Theory, percent
14.6	29.5	594	0.7062	+0.4
14.6	29.5	607	0.6950	-1.2
29.5	14.6	651	1.448	+1.8
14.6	29.5	656	0.7370	+4.8
29.5	14.6	770	1.597	+12.2

The deviation from theory in the last column is defined as:

$$\frac{\dfrac{P_{d_i}}{P_{d_f}} - \left(\dfrac{P_{h_i}}{P_{h_f}}\right)^{\frac{1}{2}}}{\left(\dfrac{P_{h_i}}{P_{h_f}}\right)^{\frac{1}{2}}}$$

from which it follows that the activation energy for diffusion of Hydrogen thru stainless steel is 13.0 kilocalories per mole.

5. CONCLUSION AND DISCUSSIONS

The principal design changes in Mark III Calibrator (relative to Mark II) were made with the expectation of achieving a well defined isothermal diffuser area, faster thermal response, and a larger dynamic range. From the linearity of Figures 8 and 12, it may be concluded that the actual diffusing area is independent of temperature and that the diffuser is isothermal. These data also imply that the diffuser hydrogen flux dynamic range is about 3×10^5 for the temperature interval $777^\circ K$ to $323^\circ K$. The latter number was defined to be the maximum spacecraft temperature and, therefore, the maximum heat sink temperature.

Data similar to that presented in Figure 16 verify that the peak pressure of a calibration pulse may be maintained for time intervals of the order of 30 seconds with less than 1.0% pressure variations, but these data also imply that separate insertion resistors are required for each calibration pulse height if in-flight step calibrations of the detector are to be performed over a relatively large dynamic range. However, if data sampling is frequent, calibration may be continuous over some specified time interval, for example, between 10 and 10^2 seconds. Thus, the full dynamic range of the diffuser may be used by fixing the diffuser heater circuit resistance such that the desired temperature rise rate is obtained for the onboard power supply available. In this continuous calibration mode, the instantaneous calibration pressure is determined from the measured instantaneous diffuser temperature and the calibration range is determined by the heating period.

For in-flight calibrations corresponding to external pressures in the mid to high pressure range of the detector, the observed pressure decay rate is such that 15 minutes after the calibration pulse the background associated with the calibration pulse (from all sources) is only a few percent of the external pressure if the calibration pulse is no more than an order of magnitude higher than the external pressure. However, near the low end of the detector pressure range, the observed decay rate

indicates that considerable attention must be given to minimization of the residual flux following a calibration pulse. The following actions are considered necessary or desirable in applications of the techniques developed here to in-flight calibration:

1) The continuous calibration mode is favored over the step calibration mode.

2) The calibration pulse height should be no larger than an order of magnitude above the external pressure near the high pressure end of the dynamic range of the detector and perhaps no more than a factor of 3 above the external pressure near the low pressure end of the detector dynamic range.

3) The calibration pulse period should be as short as possible.

4) The pumping speed of the detector should be as small as possible.

5) The external conductance should be small but large compared to the pumping speed of the detector.

6) The internal surface area of the detector should be as small as possible.

7) The diffuser area should be chosen such that the maximum calibration required is obtained only at the maximum safe diffuser temperature (probably several hundred degrees higher than the maximum temperature used here).

These actions assure that the quantity of gas liberated to produce a given height calibration pulse is minimized, that gas adsorption within the detector is minimized, and that the area of the diffuser is minimized, thus, minimizing the time required for recovery after calibration. The useful calibration pressure dynamic range achieved in a specific flight application will depend on the degree to which these requirements are satisfied.

The results obtained in this work may be summarized, for

application to the design of an in-flight calibrator, as follows: The equilibrium hydrogen flux liberated from an isothermal thin wall, 304L stainless steel diffuser tube is given by:

$$\dot{N}_{H_2} = C_1 \frac{A}{\ell} P_h^{\frac{1}{2}} \exp - \frac{C_2}{T} , \sec^{-1} ,$$

where,

$$C_1 = 2.668 \times 10^{15}, \sec^{-1} cm^{-1} Torr^{-\frac{1}{2}}$$

$$C_2 = -6608, {}^{o}K$$

$$A = \text{Area of diffuser, } cm^2$$

$$\ell = \text{Wall thickness of diffuser, cm}$$

$$P_h = \text{Hydrogen supply pressure, Torr}$$

$$T = \text{Diffuser temperature, } {}^{o}K$$

The hydrogen density within the detector enclosure is then given by:

$$n_{H_2} = \frac{\dot{N}_{H_2}}{C_{H_2}} , cm^{-3} ,$$

where, C_{H_2} = Enclosure exhaust conductance for hydrogen at the temperature of the enclosure, cm^3/sec.

Due to uncertainties in estimating the effective area for hydrogen diffusion in the diffuser used, C_1 may be in error by as much as 10%. The value of C_2 given above was taken from the high temperature portion of the data and may therefore predict a hydrogen flux, which is low at low temperatures.

REFERENCES

1. Shenker, H.; Lauritzen, J. I., Jr.; Corruccini, R. J.; and Lonberger, S. T.: Reference Tables for Thermocouples. Circular 561, National Bureau of Standards, 1955.

2. Feakes, F.; Torney, F. L., Jr.; and Brock, F. J.: Gauge Calibration Study in Extreme High Vacuum. NASA CR-167, 1965.

3. Barrer, R. M.: Diffusion In and Through Solids. Cambridge U. Press, 1941, pp. 18-19.

4. Flint, P. S.: The Diffusion of Hydrogen Through Materials of Construction. U. S. Atomic Energy Commission KAPL-659, Knolls Atomic Power Laboratory, Dec. 14, 1951.

5. Calder, R.; and Lewin, G.: Reduction of Stainless Steel Outgassing in Ultra-High Vacuum. Paper 6-6, 13th National Vacuum Symposium, American Vacuum Society, 1966.

NASA SCIENTIFIC AND TECHNICAL PUBLICATIONS

TECHNICAL REPORTS: Scientific and technical information considered important, complete, and a lasting contribution to existing knowledge.

TECHNICAL NOTES: Information less broad in scope but nevertheless of importance as a contribution to existing knowledge.

TECHNICAL MEMORANDUMS: Information receiving limited distribution because of preliminary data, security classification, or other reasons.

CONTRACTOR REPORTS: Scientific and technical information generated under a NASA contract or grant and considered an important contribution to existing knowledge.

TECHNICAL TRANSLATIONS: Information published in a foreign language considered to merit NASA distribution in English.

SPECIAL PUBLICATIONS: Information derived from or of value to NASA activities. Publications include conference proceedings, monographs, data compilations, handbooks, sourcebooks, and special bibliographies.

TECHNOLOGY UTILIZATION PUBLICATIONS: Information on technology used by NASA that may be of particular interest in commercial and other non-aerospace applications. Publications include Tech Briefs, Technology Utilization Reports and Notes, and Technology Surveys.

Details on the availability of these publications may be obtained from:

SCIENTIFIC AND TECHNICAL INFORMATION DIVISION

NATIONAL AERONAUTICS AND SPACE ADMINISTRATION

Washington, D.C. 20546